Available online at www.sciencedirect.com

ScienceDirect

Ceramics International 40 (2014) 1065–1071

CERAMICS INTERNATIONAL

www.elsevier.com/locate/ceramint

Effect of AlN–Y_2O_3 addition on the properties and microstructure of in-situ strengthened SiC–TiB_2 composites prepared by hot pressing

Jilin Hu[a,b], Hanning Xiao[a,*], Wenming Guo[a], Qing Li[a], Wen Xie[a], Baojun Zhu[a]

[a]College of Materials Science and Engineering, Hunan University, Changsha 410082, China
[b]Department of Chemistry and Materials Science, Hunan Institute of Humanities, Science and Technology, Loudi 417000, China

Received 17 May 2013; received in revised form 2 June 2013; accepted 28 June 2013
Available online 6 July 2013

Abstract

SiC–TiB_2 composites with 20 vol% TiB_2 were fabricated by in situ reaction among TiO_2, C and B_4C. Samples were densified by hot-pressing at 1900 °C with AlN and Y_2O_3 as sintering aids. The effects of the volume fraction of AlN and Y_2O_3 on the density, flexural strength, hardness and microstructure of the SiC–TiB_2 composites were determined. The results showed that SiC–TiB_2 composites possess the best comprehensive performance when the content of sintering aids is 10 vol%, at which point the relative density, flexural strength and hardness of the sintered specimens were 99.1%, 641 ± 45 MPa and 91.8 ± 0.7 HRA, respectively. The resistivity of the SiC–TiB_2 composites decreased with increasing AlN–Y_2O_3 content and reached a minimum (17.5 ± 6.7 mΩ cm) at 10 vol% AlN–Y_2O_3. Pull-out of crystal particles in the sintered body with 10 vol% AlN–Y_2O_3 was observed from the fracture morphology of the composites. Tightly bonded grains contributed to the excellent combination of properties of SiC–TiB_2 composites.

Keywords: B. Composites; Silicon carbide; Titanium diboride; Properties; Microstructure

1. Introduction

Silicon carbide (SiC) possesses an unique combination of properties, such as high temperature strength, good oxidation resistance, high thermal conductivity and extreme chemical stability, all of which make it an attractive structural material for various applications, especially those requiring abrasion resistance and high temperatures [1,2]. SiC is widely used as structural components of thermal exchangers, armour plates, cutting tools, nozzles and so on. However, the application of SiC ceramics is limited by its low room-temperature strength, poor fracture toughness and high flaw sensitivity.

An effective method to address these problems is introduction of a transition metal boride or carbide as a dispersed phase into the SiC matrix. Titanium diboride (TiB_2), one of the most important transition metal diborides discovered thus far, has attracted great interest because of its excellent properties, which include high fracture toughness, high hardness, high melting point, high electrical conductivity and considerable chemical stability [3–5]. Many reports concerning the effect of TiB_2 particles dispersed in a SiC matrix have been published [6–9].

Similar to Si_3N_4, SiC and TiB_2 are non-oxide ceramics with predominant covalent bonding; thus, they are difficult to densify without sintering additives. Densification of SiC–TiB_2 composites is usually achieved by liquid-phase sintering using Al_2O_3 and Y_2O_3 as sintering additives [6–9]. However, the commonly used additive system of Al_2O_3–Y_2O_3 does not achieve densification of SiC because the formation of gaseous products of redox reactions between SiC and Al_2O_3 is observed at sintering temperatures [10]:

$$Al_2O_3+SiC \rightarrow Al_2O(g)+SiO(g)+CO(g) \quad (1)$$

This reaction often leads to inhomogeneous microstructures, abnormal grain growth and, therefore, low reproducibility of

*Corresponding author. Tel.: +86 731 88822269; fax: +86 731 88823554.
E-mail address: hnxiao@hnu.edu.cn (H. Xiao).

0272-8842/$ - see front matter © 2013 Elsevier Ltd and Techna Group S.r.l. All rights reserved.
http://dx.doi.org/10.1016/j.ceramint.2013.06.105

mechanical properties [11]. To suppress the decomposition reaction, a powder bed with a composition similar to the sample composition is required. From a technological point of view, sintering aids should enable full densification with low mass loss and without the use of a powder bed [12]. An additive system consisting of AlN and Y_2O_3 has been found to have better sintering performance than that of Al_2O_3–Y_2O_3 when used with SiC. Unlike oxide sintering additives that tend to react with silicon carbide at sintering temperatures, which causes severe weight loss because of the formation of volatile species, addition of oxynitrides allows simpler decomposition control under nitrogen over-pressure [13–18] because the decomposition reaction

$$2AlN \rightarrow 2Al(l)+N_2(g) \quad (2)$$

is suppressed very effectively by applying a nitrogen over-pressure. Under these conditions, no powders beds are necessary for successful densification. Moreover, SiC sintered with AlN–Y_2O_3 additives has been observed to exhibit improved strength retention at high temperatures compared with conventional LPS-SiC materials [15]. Unfortunately, little research on the influence of AlN–Y_2O_3 additives on the properties and microstructure of SiC–TiB_2 composites is available.

SiC–TiB_2 composites are generally prepared by directly mixing SiC and TiB_2 powders and then hot-pressing or pressure-less sintering the powder mixture. However, mechanical mixing of the powders introduces inhomogeneity to the SiC–TiB_2 composites. In the present work, TiB_2 particles are created by internal synthesis. With TiO_2, B_4C and C as starting materials, SiC–TiB_2 composites are prepared by liquid phase sintering in a N_2 atmosphere with AlN–Y_2O_3 as additives. The mechanical properties, electrical properties and microstructure of the SiC–TiB_2 composites are also investigated in detail.

2. Experimental procedure

Commercially available α-SiC powder (purity: ≥98.5%, D_{50}=0.55 μm, D_{90}=0.79 μm, Changle Xinyuan Silicon Carbide Co., Ltd., Weifang, China), AlN powder (purity: ≥99.0%, D_{50}=0.50 μm, Shanghai Shuitian Material Science and Technology Co., Ltd., Shanghai, China), high purity Y_2O_3 powder (purity: ≥99.0%, D_{50}=3.42 μm, Ganzhou Goring High-Tech Material Co., Ltd., Ganzhou, China), sub-micrometre-scale TiO_2 powder (purity: ≥99.0%, D_{50}=1.70 μm, Shantou Guanghua Chemical Co., Ltd., Shantou, China), sub-micrometre-scale B_4C powder (purity: ≥98.0%, D_{50}=1.00 μm, Powder Metallurgy Research Institute of Central South University, Changsha, China) and high-surface area C powder (ash content: <0.1 wt%, particle size: <40 nm, Fujian Nanping Rongxin Chemical Co., Ltd., Nanping, China) were used as starting materials. The particle size distribution of α-SiC is illustrated in Fig. 1. The amounts of TiO_2, B_4C and C were adjusted to yield 20 vol% TiB_2. AlN and Y_2O_3 were used as sintering aids at a molar ratio of 3:2, and the total amounts of sintering aids added were varied to yield 5, 10, 15 and 20 vol%

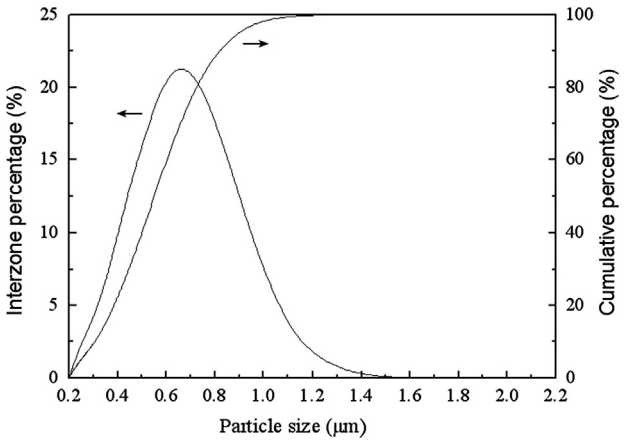

Fig. 1. The particle size distribution of α-SiC powder.

additives. The starting powders were mixed for 4 h by a planetary ball mill in a plastic jar using SiC balls as the grinding body. The well-mixed starting materials were dried at 80 °C, sieved through a 60-mesh screen and then compacted by cold uniaxial pressing at a pressure of 10 MPa into cylindrical green compacts with an approximate dimension of ∅50 mm. Sintering was performed by heating the samples to 1300 °C under vacuum for 1 h to allow the reaction among B_4C, TiO_2 and C to take place and fully convert TiO_2 to TiB_2. After 1 h, N_2 was introduced to the system. Pressure was gradually applied and the samples were heated up to the final sintering temperature. The samples were held at 1900 °C under 25 MPa for 1 h in a N_2 atmosphere before cooling.

The sintered samples were machined into rectangular bars (3 mm × 4 mm × ~35 mm), and the density of the sintered products was measured using Archimedes' method. The relative density was calculated based on the densities of SiC (3.21 g cm^{-3}), TiB_2 (4.52 g cm^{-3}), AlN (3.26 g cm^{-3}) and Y_2O_3 (5.01 g cm^{-3}) according to the rule of mixtures. Flexural strength was measured by three-point bending at 20 °C in air. The span was 30 mm and the crosshead speed was 0.5 mm/min. The hardness was determined by a digital Rockwell hardness tester. The resistivity was measured by the four-point probe method. The crystalline phases were determined by X-ray diffraction (XRD, Rigaku D/max-2200PC) using Cu-K_α radiation. The microstructures of fractured surfaces were observed by field-emission scanning electron microscopy (FE-SEM, JEOL, JSM-6700F).

3. Results and discussion

3.1. In situ synthesis principle

The in situ synthesis of TiB_2 in a SiC matrix using TiO_2, B_4C and C as the starting materials is mainly based on the following reaction:

$$2TiO_2(s)+B_4C(s)+3C(s)=2TiB_2(s)+4CO(g) \quad (3)$$

According to reaction (3), ΔG values can be calculated using the following equations:

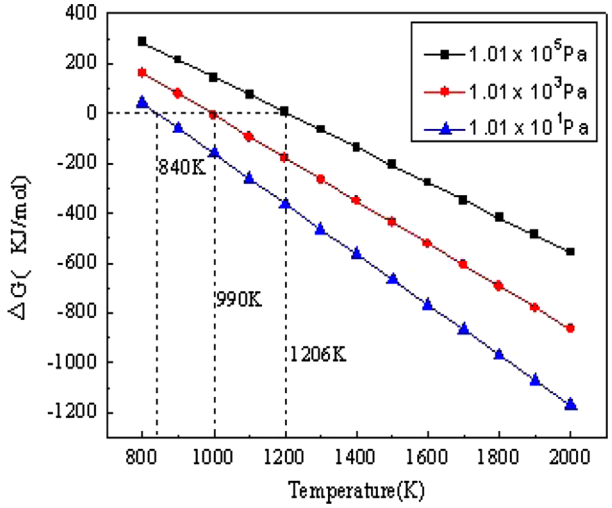

Fig. 2. The relationship between Gibbs' free energy (ΔG) and temperature (T) under different CO pressure conditions for carbothermal reduction.

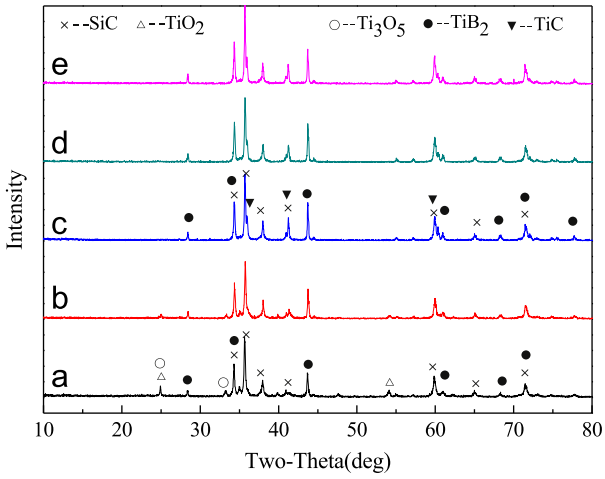

Fig. 3. XRD patterns of SiC–20 vol% TiB_2 composite powders synthesised at different temperatures under vacuum condition for 1 h: (a)1200 °C, (b) 1250 °C, (c)1300 °C, (d)1350 °C, and (e)1400 °C.

$$\Delta G = \Delta G^{\theta} + RT\ln K_{\mathrm{p}} \quad (4)$$

$$\Delta G = \Delta G^{\theta} + RT\ln(P_{\mathrm{CO}}/P^{\theta}) \quad (5)$$

$$\Delta G^{\theta} = \Delta H^{\theta} - T\,\Delta S^{\theta} \quad (6)$$

where ΔG^{θ} is the standard Gibbs free energy, R is the gas constant, K_{p} is the equilibrium constant, T is the thermodynamic temperature, P^{θ} is the standard atmospheric pressure and P_{CO} is the CO gas partial pressure.

According to the relative thermodynamics data taken from NIST-JANAF [19], the ΔG expressions can be obtained from the above equations, such that

$$\Delta G = 847{,}830 - 702.99T + 4 \times 8.314T\ln(P_{\mathrm{CO}}/P^{\theta}) \quad (7)$$

Taking P_{CO} as 1.01×10^5 Pa, 1.01×10^3 Pa, and 1.01×10^1 Pa and P^{θ} as 1.01×10^5 Pa, according to expression (7), the relationship curves between the Gibbs free energy (ΔG) and temperature (T) are shown in Fig. 2. The ΔG value decreases remarkably with increasing temperature and decreasing CO gas partial pressure, which means that temperature and CO gas partial pressure have significant effects on the synthesis of TiB_2. The results also show that the smaller the CO gas partial pressure, the larger the slope of ΔG–T. Therefore, reducing the CO gas partial pressure during the reaction is an effective method for promoting the synthesis of TiB_2. It can be inferred from the above analysis that carefully tailoring vacuum conditions will help decrease the synthesis temperature or promote the reaction to obtain TiB_2.

To investigate the effects of the reaction temperature on the synthesis of SiC–TiB_2 composite powders under vacuum conditions, SiC–20 vol%TiB_2 composite powders were synthesised in situ at temperatures ranging from 1200 °C to 1400 °C under vacuum using SiC, TiO_2, C and B_4C as starting materials. Fig. 3 shows the effects of different reaction temperatures on the phase composition of the SiC–TiB_2 composite powders. Peaks indexed to SiC and TiO_2 in the starting materials and newly formed TiB_2 and Ti_3O_5 are observed from the XRD pattern of the product treated at 1200 °C, which indicates that the carbothermal reduction of TiO_2, C and B_4C begins at 1200 °C. Peaks of TiO_2 and Ti_3O_5 gradually disappear with increasing temperature. A weak peak of TiC besides those of SiC and TiB_2 can be observed at 1300 °C in the XRD patterns. Therefore, the carbothermal reduction of the mixture may be completed at approximately 1300 °C. When the temperature is increased further to 1350 and 1400 °C, no significant changes in the XRD patterns are observed but the diffraction peaks of SiC and TiB_2 become more intense. Such a pattern indicates that the composite powders obtained at 1350 and 1400 °C possess increased crystallinity.

Because CO, a by-product of the synthesis of TiB_2, must dissipate so that the reaction can continue, ignition loss can be used as an indicator of the reaction process. A greater ignition loss implies a higher degree of completion of the reaction. In this study, the ratio of the actual ignition loss to the theoretical ignition loss (the relative ignition loss) was used to determine the degree of completion of the reaction. The relationship between relative ignition loss and reaction temperature for the products is shown in Fig. 4. The relative ignition loss increases when the heating temperature is increased, reaching 75.99% and 91.01% at 1200 and 1250 °C, respectively. The relative ignition loss rises to 106.42% when the temperature is increased to 1300 °C. As the temperature is further increased to 1350 and 1400 °C, the relative ignition loss increases by only 2.13% and 3.66%, respectively. These results strongly suggest that carbothermal reduction is completed at 1300 °C, which is in accordance with the XRD analysis results. The higher relative ignition loss compared with the theoretically calculated value at above 1300 °C may be explained as follows [20,21]: as an intermediate in the synthesis of TiB_2 from TiO_2 and B_4C, B_2O_3 has an unusually low melting point (450 °C) and a high vapour pressure. It is volatile at high temperatures under vacuum, and a very small amount of the intermediate may be removed with the

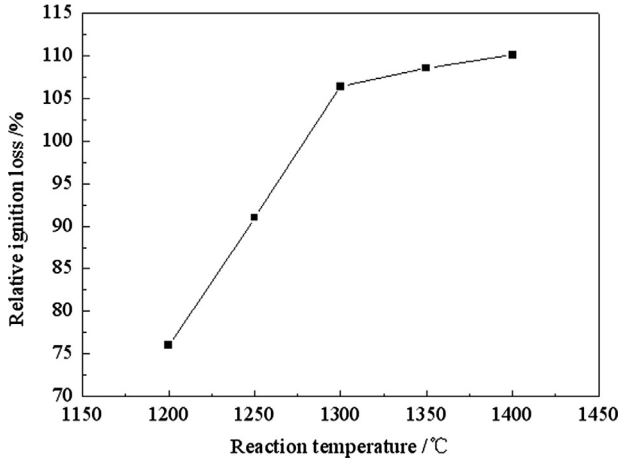

Fig. 4. The relationship between relative ignition loss and reaction temperature for the products.

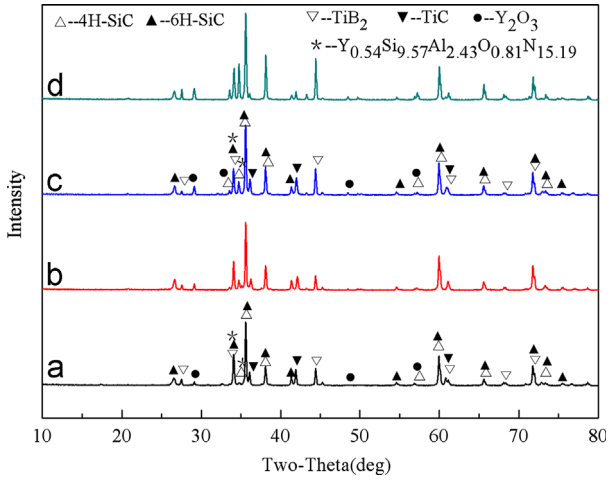

Fig. 5. XRD patterns of sintered samples with different volume fractions of sintering aids: (a) 5 vol%, (b) 10 vol%, (c) 15 vol%, and (d) 20 vol%.

CO gas. This phenomenon may cause the actual relative ignition loss to become higher than the theoretically calculated value.

During the synthesis of SiC–TiB_2 composite powders, the following reactions may occur [20,22–24]:

$$7TiO_2(s)+5B_4C(s)=7TiB_2(s)+3B_2O_3(l)+5CO(g) \quad (8)$$

$$TiO_2(s)+B_2O_3(l)+5C(s)=TiB_2(s)+5CO(g) \quad (9)$$

$$3TiO_2(s)+C(s)=Ti_3O_5(s)+CO(s) \quad (10)$$

$$Ti_3O_5(s)+8C(s)=3TiC(s)+5CO(s) \quad (11)$$

$$TiC(s)+B_2O_3(l)+2C(s)=TiB_2(s)+3CO(g) \quad (12)$$

TiB_2 is directly synthesised by TiO_2 and B_4C or by B_2O_3 generated from reaction (8), TiO_2 and C. TiB_2 can also be converted from TiC generated by the reaction of TiO_2 and C. Dissipation of a small amount of the intermediate B_2O_3 means that the excess TiO_2 and C can form TiC based on reactions (10) and (11). That is, a small amount of TiC in the synthesised products may not be completely converted into TiB_2, as confirmed by the XRD analysis. Therefore, the presence of TiC in the synthesised powder is mainly attributed to the vaporisation and removal of B_2O_3.

3.2. Phase composition

The XRD patterns of sintered samples with different volume fractions of sintering aids are shown in Fig. 5. The major phase of the sintered specimens is α-SiC (4H or 6H) and the minor phase is TiB_2; trace phases, such as those of TiC, $Y_{0.54}Si_{9.57}Al_{2.43}O_{0.81}N_{15.19}$ and Y_2O_3, may also be observed. The figure demonstrates that the intensities of the diffraction peaks of α-SiC and TiB_2 increase with increasing content of sintering aids, as obviously shown in the pattern obtained at 2θ of 25–45°. Because AlN powder possesses high purity, no $Y_3Al_5O_{12}$ intergranular phase is generated from the reaction of Al_2O_3 and Y_2O_3. A small amount of TiC in the SiC–TiB_2 composites has a positive effect on the mechanical and thermal properties of the resulting products because TiC possesses an excellent combination of high fracture toughness, high melting point (~3000 °C), high Vickers hardness (28–35 GPa), excellent chemical stability and good oxidation resistance at high temperatures. Therefore, SiC–TiB_2 composites containing TiC may be excellent materials for future applications, presenting combined properties of high temperature strength, good oxidation resistance, high hardness and high thermal conductivity.

Table 1
The density of the SiC–TiB_2 composites.

Sample	Volume fraction of sintering aids (%)	Sintered density (g cm^{-3})	Theoretical density (g cm^{-3})	Relative density (%)
ST-5	5	3.36	3.52	95.5
ST-10	10	3.54	3.57	99.1
ST-15	15	3.57	3.63	98.3
ST-20	20	3.61	3.68	98.1

3.3. Densification

The effect of volume fraction of sintering aids on the density of the SiC–20 vol%TiB_2 composites is presented in Table 1. The density of the sintered samples increases with increasing volume fraction of sintering aids and reaches a maximum at a certain volume fraction. The relative density of the samples sintered at 1900 °C is 95.5% when the volume fraction of the sintering aids is 5 vol%. The maximum relative density is observed from the samples with 10 vol% sintering aids at 1900 °C. At this temperature, the density of sample ST-10 is 3.6% higher than that of sample ST-5, which means that sintering aids containing AlN and Y_2O_3 can effectively improve the sintering of SiC–TiB_2 composites. Both SiC and AlN have a hexagonal crystal structure and approximate lattice parameters. Although SiC and AlN have strong covalent bonds, they can form a solid solution in a wider range of compositions and temperatures because of the similarities in

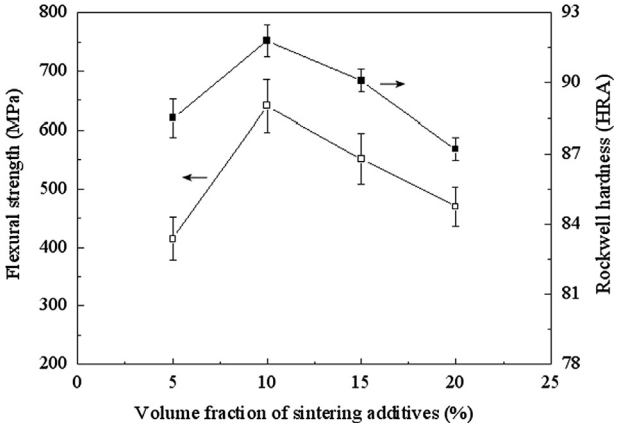

Fig. 6. The effect of volume fraction of sintering additives on the flexural strength and hardness of the samples sintered at 1900 °C.

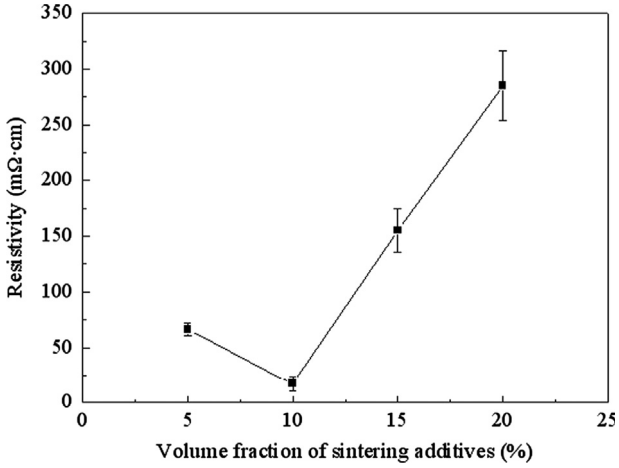

Fig. 7. The effect of volume fraction of sintering additives on the resistivity of the samples sintered at 1900 °C.

their crystal structure [25–27]. The formation of a solid solution between SiC and AlN contributes to the reduction of their respective boundary energies, thereby promoting the displacement and migration of Si, C, Al and N atoms in the lattice and improving the sintering property of the materials. In addition, AlN–Y_2O_3 system phase diagrams [14] show that the liquid phase of composites formed at high temperature increases linearly with increasing content of sintering aids, which accelerates the rearrangement of SiC and TiB_2 particles as well as the dissolution and reprecipitation process accompanied by substance migration and promotes the combination of reinforcement and matrix materials. However, as the amount of sintering aids added to the system continues to increase, the relative density of SiC–TiB_2 composites decreases. When the amount of sintering aids added reaches 15 and 20 vol%, the relative density of the SiC–TiB_2 composites decreases to 98.3% and 98.1%, respectively. Such behaviour may be explained as follows: the effect of the liquid phase on the densification of the materials during sintering is focused on accelerating the sintering process during the early-to-middle stages of sintering; in the late stage of sintering (especially at density > 95%), densification of the materials is mainly completed by volume diffusion of the grain boundary, and the liquid phase has little effect on densification. The excess liquid phase can increase the growth of the grains and thus affect the properties of the SiC–TiB_2 composites.

3.4. Mechanical properties

Fig. 6 shows the correlation between the mechanical properties of the SiC–TiB_2 composites and their content of sintering aids. The flexural strength of the SiC–TiB_2 composites improves significantly as the content of sintering aids increases, increasing from 415 ± 36 MPa to 641 ± 45 MPa as the content of sintering aids increases from 5 vol% to 10 vol%. This increase in flexural strength may be attributed to three factors: first, the liquid phase produced by the sintering aids can promote densification of the sintered samples, thereby improving their mechanical properties. Second, addition of AlN refines the grains [28], which also improves the mechanical properties of the samples. Finally, insertion of soft-phase AlN into the hard-phase SiC lattice may contribute to the mechanical properties of the products. However, excess addition of sintering aids may accelerate grain growth and thus decrease the flexural strength of the sintered bodies.

As shown in Fig. 6, the change in hardness shows a trend similar to that of flexural strength with increasing AlN–Y_2O_3 content. The Rockwell hardness of the samples increases with increasing AlN–Y_2O_3 contents, reaching a maximum value at 10 vol% AlN–Y_2O_3 and then gradually decreasing at 15 and 20 vol% AlN–Y_2O_3. This behaviour may be explained by the fact that both AlN and Y_2O_3 have theoretically lower hardness than SiC and TiB_2. Specific amounts of sintering aids can promote densification of the sintered bodies, which, in turn, contributes to the hardness of the resulting specimens.

3.5. Electrical properties

The effect of volume fraction of sintering additives on the resistivity of SiC–TiB_2 composites sintered at 1900 °C is presented in Fig. 7. The resistivity of the SiC–TiB_2 composites decreases with increasing AlN–Y_2O_3 content and reaches a minimum of 17.5 ± 6.7 mΩ cm at 10 vol% AlN–Y_2O_3. Two key factors affect electrical conductivity: the number of conductive particles and the shortest distance amongst particles [29,30]. In SiC–TiB_2 composites containing AlN and Y_2O_3, SiC, AlN and Y_2O_3 show poor electrical conductivity, whereas TiB_2 shows favourable conductivity. Hence, conductive particles within the samples are mainly TiB_2 particles formed at high temperature. When the content of AlN and Y_2O_3 is low (≤10 vol%), the liquid phases generated from the AlN–Y_2O_3 particles reduce the voids in the system and increase its density. Furthermore, conductive particles achieve favourable contact and the conductive path is shortened. Thus, the resistivity of SiC–TiB_2 composites decreases with increasing AlN–Y_2O_3 contents but increases when AlN–Y_2O_3 is over

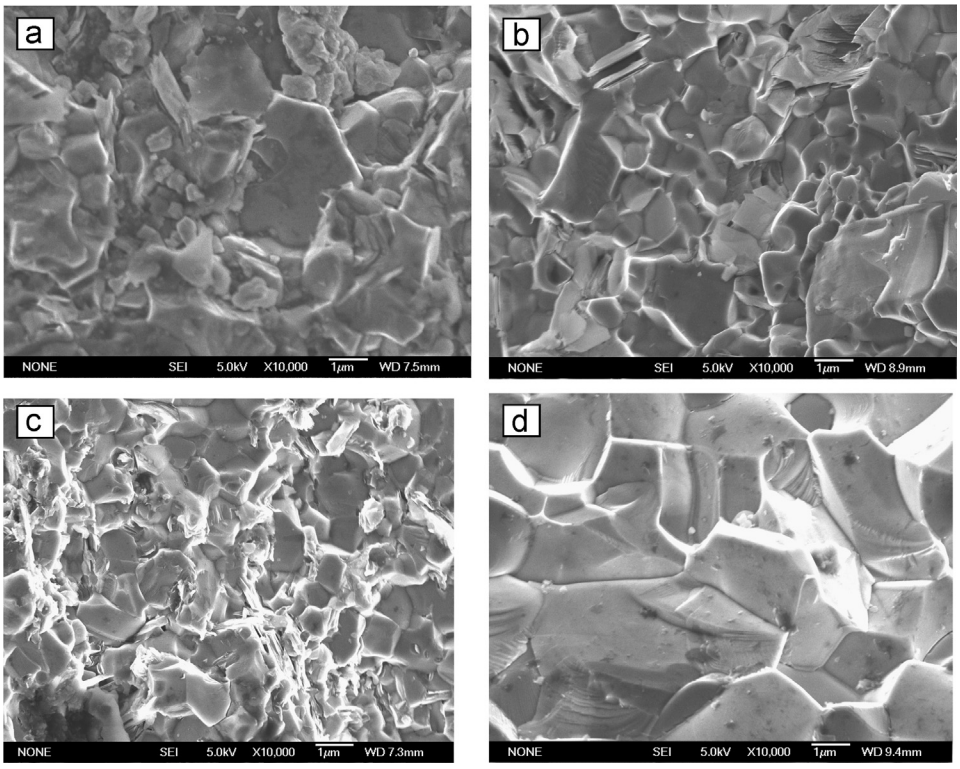

Fig. 8. The fracture morphologies of SiC–TiB_2 composites containing 5 – 20 vol% sintering aids obtained by hot pressing at 1900 °C for 1 h: (a) 5 vol%, (b) 10 vol %, (c) 15 vol%, and (d) 20 vol%.

15 vol%. This change in resistivity may be explained by excess sintering additives slightly increasing the porosity and decreasing the density of the sample.

3.6. Microstructure

Fig. 8 shows the fracture morphologies of SiC–TiB_2 composites containing 5 – 20 vol% sintering aids obtained by hot pressing at 1900 °C for 1 h. When the content of sintering aids is low (5 vol %), the fracture surface of the specimen is characterised by a combination of mostly intergranular brittle regions and a few cleavage regions. The region between the reinforcement material and the matrix is prone to cracks and large gaps, which implies a weak interface between the two. The density of the SiC–TiB_2 composites increased with increasing sintering aid content, indicating strengthening of the interface between the reinforcement material and the matrix. Fig. 8(b) shows traces of grain pull-out and tight bonding of crystals, which improves the flexural strength of the specimens. Therefore, SiC–TiB_2 composites with 10 vol% sintering aids possess excellent flexural strength, high hardness and low resistivity. When the added amount of sintering aids reaches 15 vol%, the fracture surface of the specimen is relatively smooth (Fig. 8(c)). A large amount of the liquid phase gathers on the grain interface and holes begin to appear on the surface of the sample, thereby decreasing the flexural strength and increasing the resistivity of the sample. Further increase in the content of sintering aids (20 vol%) causes the grain size of the specimens (Fig. 8(d)) to increase significantly, which has a harmful effect on the mechanical and electrical properties of the samples.

4. Conclusions

Choosing appropriate vacuum conditions can decrease the synthesis temperature and promote the in situ synthesis of TiB_2 from TiO_2, C and B_4C. The carbothermal reduction of a mixture of these materials may reach completion at approximately 1300 °C under vacuum conditions. As some B_2O_3 is removed from the system at high temperatures, a small amount of TiC is observed in the synthesised products, resulting in a higher relative ignition loss than that theoretically calculated.

The major phases of the sintered specimens are α-SiC and TiB_2; trace phases of TiC, AlN and Y_2O_3 may also be observed. The relative density, flexural strength and Rockwell hardness of sintered samples with 10 vol% sintering aid content reach maximum values of 99.1%, 641 ± 45 MPa and 91.8 ± 0.7 HRA, respectively. The resistivity of the SiC–TiB_2 composites decreases with increasing AlN–Y_2O_3 content, reaches a minimum of 17.5 ± 6.7 mΩ cm at 10 vol% AlN–Y_2O_3 and then gradually increases at 15 and 20 vol% AlN–Y_2O_3.

At a sintering aid content of 5 vol%, the fracture surface of the specimen is characterised by a combination of mostly intergranular brittle regions and a few cleavage regions. Grain pull-out is observed at 10 vol% sintering aid content. At higher sintering aid contents (≥15 vol%), the fracture surface is relatively smooth and some pores may be observed.

Acknowledgements

The authors thank the National Science Foundation of China (Grant no. 50972042) for their support of this research.

References

[1] X. Xu, S. Mei, J.M.F. Ferreira, T. Nishimura, N. Hirosaki, Silicon carbide ceramics through temperature-induced gelation and pressureless sintering, Materials Science and Engineering A 382 (1–2) (2004) 335–340.

[2] K.Z. Li, J. Wei, H.J. Li, C. Wang, G.S. Jiao, Silicon assistant carbothermal reduction for SiC powders, Journal of University of Science and Technology Beijing 15 (4) (2008) 484–488.

[3] M.K. Ferber, P.F. Becher, C.B. Finch, Effect of microstructure on the properties of TiB_2 ceramics, Journal of the American Ceramic Society 66 (1) (1983) C-2–C-3.

[4] M.J. Edirisinghe, J.I. Mccollum, History and recent development in SHS, Ceramics International 19 (1993) 113–120.

[5] S.H. Kang, D.J. Kim, Synthesis of nano-titanium diboride powders by carbothermal reduction, Journal of the European Ceramic Society 27 (2) (2007) 715–718.

[6] D. Bucevac, S. Boskovic, B. Matovic, V. Krstic, Toughening of SiC matrix with in-situ created TiB_2 particles, Ceramics International 36 (2010) 2181–2188.

[7] D. Bucevac, B. Matovic, S. Boskovic, S. Zec, V. Krstic, Pressureless sintering of internally synthesised SiC–TiB_2 composites with improved fracture strength, Journal of Alloys and Compounds 509 (2011) 990–996.

[8] S.S. Ordan'yan, S.V. Vikhman, É.V. Prilutskii, Investigation of the structure and properties of materials in the SiC–TiB_2 system, Powder Metallurgy and Metal Ceramics 41 (1–2) (2002) 42–46.

[9] K.S. Cho, H.J. Choi, J.G. Lee, Y.W. Kim, Effects of additive amount on microstructure and fracture toughness of SiC–TiB_2 composites, Ceramics International 24 (4) (1998) 299–305.

[10] M.A. Mulla, V.D. Krstic, Pressureless sintering of β-SiC with Al_2O_3 additions, Journal of Materials Science 29 (4) (1994) 934–938.

[11] V.A. Izhevskyi, A.H.A. Bressiani, J.C. Bressiani, Effect of liquid phase sintering on microstructure and mechanical properties of Yb_2O_3–AlN containing SiC-based ceramics, Journal of the American Ceramic Society 88 (5) (2005) 1115–1121.

[12] G. Rixecker, I. Wiedmann, A. Rosinus, F. Aldinger, High-temperature effects in the fracture mechanical behaviour of silicon carbide liquid-phase sintered with AlN–Y_2O_3 additives, Journal of the European Ceramic Society 21 (2001) 1013–1019.

[13] M. Nader, F. Aldinger, M.J. Hoffmann, Influence of the α/β-SiC phase transformation on microstructural development and mechanical properties of liquid phase sintered silicon carbide, Journal of Materials Science 34 (6) (1999) 1197–1204.

[14] K. Biswas, Liquid Phase Sintering of SiC Ceramics with Rare Earth Sesquioxides, Doctoral Thesis, University of Stuttgart, 2003.

[15] K. Biswas, G. Rixecker, I. Wiedmann, M. Schweizer, G.S. Upadhyaya, F. Aldinger, Liquid phase sintering and microstructure–property relationships of silicon carbide ceramics with oxynitride additives, Materials Chemistry and Physics 67 (1) (2001) 180–191.

[16] L.K.L. Falk, Imaging and microanalysis of liquid phase sintered silicon-based ceramic microstructures, Journal of Materials Science 39 (22) (2004) 6655–6673.

[17] K. Suzuki, M. Sasaki, Microstructure and mechanical properties of liquid-phase-sintered SiC with AlN and Y_2O_3 additions, Ceramics International 31 (5) (2005) 749–755.

[18] K. Strecker, M.J. Hoffmann, Effect of AlN-content on the microstructure and fracture toughness of hot-pressed and heat-treated LPS-SiC ceramics, Journal of the European Ceramic Society 25 (6) (2005) 801–807.

[19] M.W. Chase Jr., NIST-JANAF Thermochemical Tables, 4th ed., Journal of Physical and Chemical Reference Data, Monograph 9, 1998.

[20] W.M. Guo, G.J. Zhang, Reaction processes and characterization of ZrB_2 powder prepared by boro/carbothermal reduction of ZrO_2 in vacuum, Journal of the American Ceramic Society 92 (1) (2009) 264–267.

[21] W.G. Fahrenholtz, The ZrB_2 volatility diagram, Journal of the American Ceramic Society 88 (12) (2005) 3509–3512.

[22] T. Saito, T. Fukuda, H. Maeda, K. Kusakabe, S. Morooka, Synthesis of ultrafine titanium diboride particles by rapid carbothermal reduction in a particulate transport reactor, Journal of Materials Science 32 (15) (1997) 3933–3938.

[23] N.A. Hassine, J.G.P. Binner, T.E. Cross, Synthesis of refractory metal carbide powders via microwave carbothermal reduction, International Journal of Refractory Metals and Hard Materials 13 (6) (1995) 353–358.

[24] H. Preiss, L.M. Berger, D. Schultze, Studies on the carbothermal preparation of titanium carbide from different gel precursors, Journal of the European Ceramic Society 19 (2) (1999) 195–206.

[25] G. Magnani, L. Beaulardi, A. Brentari, T. Toyoda, K. Takahashi, Crack healing in liquid-phase-pressureless-sintered silicon carbide–aluminum nitride composites, Journal of the European Ceramic Society 30 (3) (2010) 769–773.

[26] A. Zangvil, R. Ruh, Phase relationships in the silicon carbide–aluminum nitride system, Journal of the American Ceramic Society 71 (10) (1988) 884–890.

[27] Y.W. Kim, M. Mitomo, T. Nishimura, Heat-resistant silicon carbide with aluminum nitride and erbium oxide, Journal of the American Ceramic Society 84 (9) (2001) 2060–2064.

[28] Z.M. Chen, S.H. Tan, D.L. Jiang, High performance SiC–AlN composites, Journal of Inorganic Materials 12 (5) (1997) 763–767.

[29] Z.D. Guan, Z.T. Zhang, J.S. Jiao, Physical Properties of Inorganic Materials, Tsinghua University Press, Beijing, China, 2001.

[30] W.Z. Jiang, Carbon Technology, Metallurgical Industry Press, Beijing, China, 2009.